

MARTIAN MESOSPHERIC CO₂ CLOUDS & GRAVITY WAVE ACTIVITY.

A. Spiga^{1,2}, F. Gonzalez-Galindo^{2,1}, F. Forget¹, M.-A. Lopez-Valverde², ¹Laboratoire de Météorologie Dynamique, Université Pierre et Marie Curie, France, ²Instituto de Astrofísica de Andalucía, Consejo Superior de la Investigación Científica, Spain.

Introduction and background

When topography, convection or wind shear perturb the stratified atmospheric fluid, the buoyancy restoring force causes oscillations called gravity waves (GW, cf. review by Fritts and Alexander, 2003). Typical horizontal scales of such phenomena range from thousands of kilometres to few kilometres. GWs are ubiquitous in the Martian low-density stable atmosphere (e.g. Creasey et al., 2006). Clouds shaped by GW propagation were one of the first dynamical phenomena monitored by spacecraft orbiting Mars (Briggs and Leovy, 1974).

Of particular interest are the vertically-propagating GWs emitted in the lowermost atmospheric levels, which amplitude increases exponentially as density decreases in the rarefied upper layers of the Martian atmosphere. The propagation and/or breaking of those waves yield local temperature and momentum disturbances at altitudes above ~ 60 km (detected in entry profiles, e.g. Magalhães et al., 1999; Withers and Catling, 2010). Such disturbances are known to impact the large-scale circulations, hence it is necessary to include parameterizations in Martian Global Circulation Models [GCMs] which are not able to resolve fine-scale GWs.

At about same altitudes in the mesosphere / thermosphere, detached hazes thought to be composed of CO₂ ice particles were discovered a decade ago through ground-based spectroscopy and Pathfinder observations (Clancy and Sandor, 1998). These pioneering observations were later confirmed by observations both on board Mars Global Surveyor using TES (MEM clouds, Clancy et al., 2007) and THEMIS (McConnochie et al., 2010) instruments, and Mars Express using SPICAM (Montmessin et al., 2006), OMEGA (Montmessin et al., 2007) and HRSC (Määttänen et al., 2010) instruments. These recent studies provided details on the morphology, the preferred regions of occurrence and the seasonal variability of mesospheric CO₂ clouds.

Clancy and Sandor (1998) speculated that *CO₂ ice clouds should form within the temperature minima of tidal and GWs in the Mars mesosphere and be fairly common phenomena at low-to-mid latitudes during day / night times.* The tidal influence has been recently analyzed by González-Galindo et al. (2011) [cf. also in this issue]. Here we use CO₂ clouds observations and numerical simulations to explore links between CO₂ clouds and GW activity in the Martian mesosphere. We show that GWs are one of the key elements needed to answer the following questions: 1. What are the atmospheric dynamical

processes responsible for the formation of mesospheric CO₂ clouds? 2. How the observed spatial and temporal variability of those clouds could be accounted for?

CO₂ clouds and GW-induced cold pockets

Thus far, the variability of CO₂ clouds has been mostly examined through GCM studies. GCMs cannot resolve most GWs, but instead yield useful arguments to account for the spatial and temporal variability of mesospheric CO₂ clouds and associated high-altitude cold conditions (Montmessin et al., 2007; Määttänen et al., 2010). Preferential formation of CO₂ clouds near the equator and at local time 16 : 00 can be explained by coldest mesosphere at altitudes 60 – 90 km in the end of the afternoon, owing to propagating thermal tides (González-Galindo et al., 2011). Nevertheless, the predicted temperatures in the GCM at those local times and altitudes are still 5 – 10 K warmer than the CO₂ condensation point. Here we want to test if unresolved mesoscale circulations (namely, GWs) play an important role in the formation of CO₂ clouds as a necessary complement to favourable large-scale conditions.

Our approach is to use mesoscale modeling with high-resolution temporal, spatial and vertical resolution to better constrain the characteristics of Martian GWs. Starting from existing and validated tools, we built a “whole atmosphere” model extending from the Martian surface to the upper thermosphere. The model consists of the Spiga and Forget (2009) mesoscale model with full physical parameterizations for Mars, where the latest parameterizations for radiative transfer in the thermosphere have been activated (González-Galindo et al., 2009). The 3D model described in Spiga and Forget (2009) is run here in bidimensional mode: along the horizontal dimension, we set idealized gaussian topography and incoming flow; along the vertical, we set a 50 km-deep sponge layer at the top located around 180 km altitude. Hence the model is designed to be an idealized “GW numerical laboratory”, allowing GWs to propagate from realistic tropospheric sources to mesospheric environments prone to complex radiative processes.

Our “whole atmosphere” model is an improvement to the existing models described in the literature, which employ either imposed GW spectra, *ad hoc* wave packet in a simple 1D vertical propagation model (Parish et al., 2009), or troposphere-only vertical extent. The rationale for 2D simulations is low computational time, which

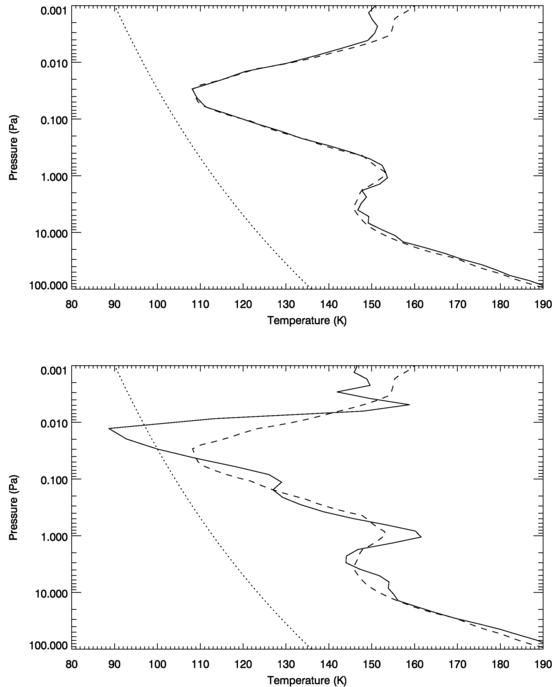


Figure 1: Perturbations of atmospheric temperature caused by vertical propagation of GWs. Simulations carried out at $L_s = 0^\circ$, latitude $\varphi = 0^\circ$, longitude $\lambda = 0^\circ$, around local time 16:00, when mesospheric CO₂ clouds have been observed at altitudes 70-80 km by the Mars Express / OMEGA spectrometer. Outputs from idealized mesoscale modeling (MM, full line) initialized with results from general circulation modeling (GCM, dashed line). While GCM computations do not predict conditions for CO₂ condensation, high-resolution MM computations yield temperatures below CO₂ condensation level (dotted lines) at altitudes where CO₂ clouds have been observed.

permits numerous experiments with various mountain sizes and incoming flow characteristics [fewer 3D experiments were carried out to verify that 2D simulations captured key features]. The model is initialized with GCM profiles extracted from simulations performed for the Määttänen et al. (2010) and González-Galindo et al. (2011) studies.

Results from the model for mountain height of 4 km and incoming wind of 15 m s^{-1} are shown in Figure 1 after three hours of integration. An xz slice of vertical velocity features the well-known mountain wave perturbation with alternating oblique patterns of positive and negative vertical velocity, reaching 6 m s^{-1} in the higher atmosphere: Figure 1 corresponds to a vertical profile of temperature on a grid point over which high perturbations of vertical wind are reached. It is expected from theory that temperature perturbations caused by GW propagation amplify with altitude as density decreases. The model shows that the amplitude of temperature perturbations can reach a few tens of kelvins

at the altitude where the GCM minimum of temperature is occurring ($\sim 70 - 80 \text{ km}$), thereby causing temperature to fall below the CO₂ condensation values over a depth roughly similar to what was inferred for the CO₂ cloud layer by Montmessin et al. (2007). The order of magnitude for temperature departures is consistent with temperature fluctuations observed in e.g. the Pathfinder entry profiles, speculated to be caused by GW propagation (Magalhaes et al., 1999). Note that the CO₂ condensation scheme in the Spiga and Forget (2009) model is switched off in the present numerical experiments to allow for the development of mesospheric supercold pockets below the CO₂ condensation temperature as in Figure 1. The mesoscale model predicts significant departures (at least 5 K) below the condensation point, which posits significant latent heat release and possible deep convective conditions. However, such process would depend strongly on the ratio between the characteristic timescale for GW propagation and the characteristic timescale for speculated deep convection involving CO₂ [cf. Määttänen et al., this issue]. Note also that our model does not attempt to couple GW dynamics to CO₂ microphysics, which is left as future work. Here we show only one component of the “recipe” to create high-altitude CO₂ clouds: that GW-induced supercold pockets are making Martian mesosphere a favourable host for those phenomena.

Variability of CO₂ clouds and GW filtering

The numerical experiments described in the previous section aimed at studying realistic GWs propagating in the upper atmosphere. Results in Figure 1 were shown for a case where wind is assumed constant along the vertical. Simulations with various wind profiles were also carried out and showed (as could be expected from theory) that vertical variations of horizontal wind could impact significantly GW propagation. As was stated by Lindzen (1981) in a seminal paper about terrestrial GWs, *winds in the troposphere and the stratosphere sharply limit the phase speeds of waves capable of reaching the upper mesosphere*. This is especially critical in this study since observations of mesospheric CO₂ clouds are usually associated with strong winds, easterlies for most equatorial clouds (Määttänen et al., 2010; McConnochie et al., 2010). Hence vertical profiles of stability and horizontal wind must be analyzed to assess if the GW might encounter either breaking or critical level before reaching the 60–80 km altitudes. A critical level is reached when the GW could no longer physically propagate because its phase speed has reached the speed of the mean flow in which it is propagating.

Thus, a second step after our idealized simulations is to determine locations where, and seasons when, GWs emitted in the troposphere would be able to propagate in the thermosphere to form supercold pockets favourable

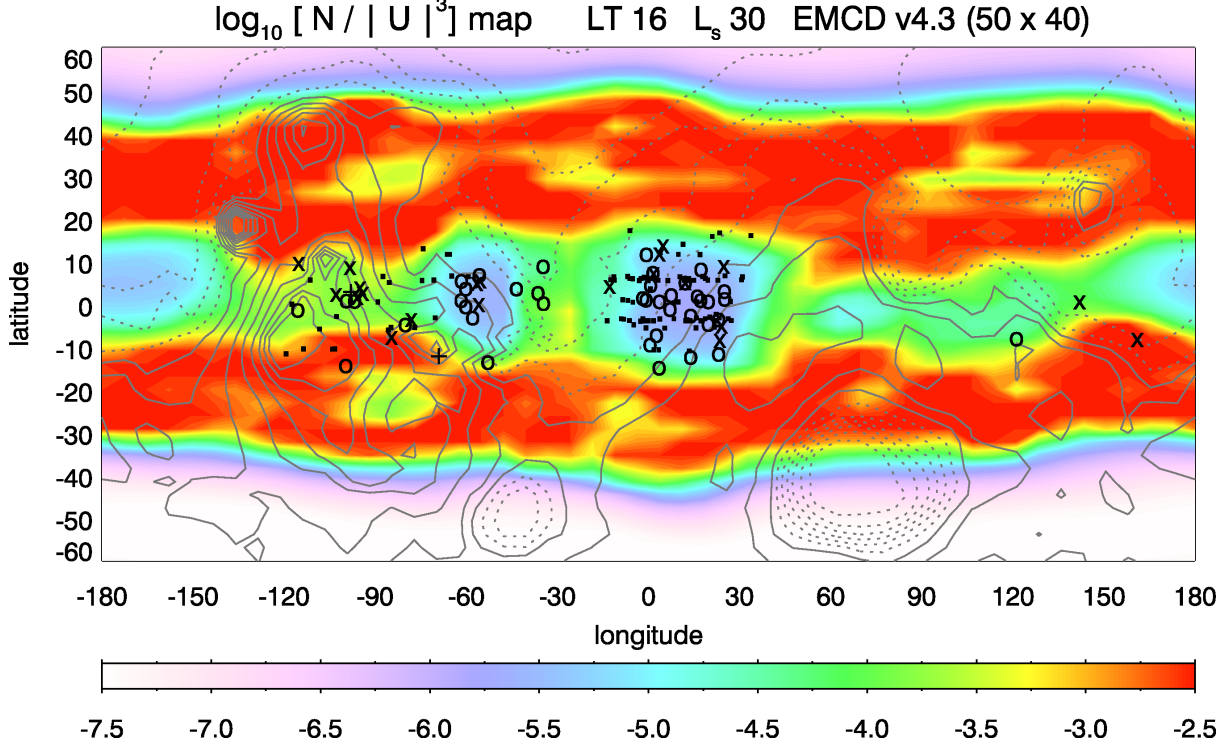


Figure 2: Maps of maximum $\frac{N}{|U|^3}$ reached between $30 < z < 90$ km at local time 16 : 00 and $L_s = 30^\circ$, using MCD climatologies. Pale purple to blue areas in the figures correspond to regions where GW activity is likely to be found at mesospheric altitudes for vertically-propagating waves are less likely to having been filtered out by critical layers or wave breaking. The observations of afternoon mesospheric CO₂ clouds (either putative or detected) at altitudes between $55 < z < 90$ km and $0^\circ < L_s < 70^\circ$ obtained by TES [·], OMEGA [○], HRSC [×] and THEMIS [+] are superimposed.

to CO₂ cloud formation. To answer this question, we carried out a specific study using Mars Climate Database climatologies (MCD, e.g. Millour et al., 2008) to characterize the mean state of the Martian atmosphere all over the planet and throughout the year, in a nominal non-dusty scenario. GW breaking and critical levels occur in specific wind and stability conditions. A fair amount of terrestrial studies have been dedicated to the topic; we used the simple yet powerful criterion built by Hauchecorne et al. (1987) to estimate GW saturation at high altitudes:

$$R_{\text{sat}} = \frac{T'}{T'_{\text{sat}}} = \sqrt{\frac{F_0}{\rho k_x} \frac{N}{|U - c|^3}}$$

where z is the altitude above the surface, $T'(z)$ is the GW-induced temperature perturbation, $T'_{\text{sat}}(z)$ the maximum perturbation before the wave reaches critical level, F_0 the GW vertical momentum flux (a constant according to the Eliassen-Palm theorem), k_x the horizontal wavenumber, $N(z) = \sqrt{g/\theta} \times d\theta/dz$ the atmospheric stability, $\rho(z)$ the atmospheric density, $U(z)$ the background wind, c the GW phase speed. The closer R_{sat} to 1, the highest probability a GW propagating from the troposphere to the mesosphere would be filtered out. Or,

low R_{sat} means GW propagation with lower likelihood of encountering breaking or critical level. Environmental atmospheric conditions are expressed through the term indicated in red in the formula. To apply this formula to Mars, we consider for simplicity only mountain waves with $c \sim 0 \text{ m s}^{-1}$. Those can be considered to virtually appear in any Martian regions at any season, while other sources (fronts, dust storms) are much more localized in space and time. There is an exception though with GWs generated by boundary layer convection (Spiga and Forget, 2009), which might occur everywhere, but such waves are analogous to mountain waves through the “obstacle effect”.

As shown in Figure 2, we built maps of $\frac{N}{|U|^3}$ from MCD predictions. We display the maximum value reached between $30 < z < 90$ km (below 30 km is the place for mesoscale perturbations to be generated, so we assume that at least wave packets are able to make it through this layer). Pale purple to blue areas in the figure point toward regions where GW activity is likely to be found at mesospheric altitudes (where clouds would be observed), because GW vertical propagation has not been annihilated by critical layers or wave breaking. Inspection of typical vertical profiles of wind shows that the limiting factor is usually when the jet speed decreases

REFERENCES

towards 0 m s^{-1} and critical layer appears, which leads to high N/U^3 . As far as low N/U^3 values are concerned, those correspond to either strong westerlies or easterlies all over the considered vertical column without any wind inversion.

Is there a correlation between regions/seasons where and when GW are left unfiltered and free to propagate vertically (low $\frac{N}{U^3}$) and the appearance of CO_2 clouds in the Martian mesosphere? The longitude/latitude map in Figure 2 shows the particular case of clouds observed in northern spring (around $L_s = 30^\circ$, at the season when lots of high hazes have been reported). The two main “clusters” of clouds over Terra Meridiani and Valles Marineris / Tharsis, as well as the few clouds around Elysium Mons, correspond to low values of N/U^3 . This supports the hypothesis that GW activity has a significant influence on the occurrence of mesospheric CO_2 clouds. Those clouds are possibly more likely to appear when and where stability and wind conditions allow for GWs to propagate high in the Martian atmosphere without encountering saturation or critical levels. Only a few observed cloud events are located in areas with high N/U^3 , which can be regarded as acceptable given the known MCD uncertainties [Millour et al., this issue]. The seasonal variability of CO_2 clouds is also correctly accounted by the saturation criterion (figures not shown here for the sake of brevity). Areas with particularly low saturation ratio (hence favoured GW vertical propagation) are associated with winter mid-latitude jets (consistently with wind speeds and directions inferred from CO_2 cloud observations) and solstice tide maxima.

Conclusion

The conclusions of our work are the following

1. Cold mesospheric perturbations caused by vertically-propagating mesoscale GWs on Mars can reach few tens of K at altitudes 60–90 km, hence appear key to the formation of CO_2 clouds (complementary to large-scale processes).
2. Regions and seasons where / when CO_2 clouds are observed are characterized by favourable atmospheric conditions for GW propagation (in the sense of saturation and critical levels).

This work is only a step towards fully understanding the formation of high-altitude CO_2 clouds in the Martian atmosphere. Dynamical insights must be gained on potential wave-wave interactions between thermal tides and GWs, on coupling between radiative, microphysical and dynamical processes. At the same time, our work also shows that CO_2 clouds have the potential to be a revelator of the numerous subtleties of the Martian low-density atmospheric dynamics.

Acknowledgements We warmly thank A. Määttänen, S. R. Rafkin, F. Montmessin, R. T. Clancy, P. Withers for helpful discussions. We acknowl-

edge Junta de Andalucía for “visiting scientist” grant, as well as IPSL, ESA and CNES for support through research grants and contracts.

References

- Briggs, G. A. and Leovy, C. B. (1974). Mariner 9 observations of the Mars north polar hood. *Bull. Am. Meteorol. Soc.*, 55:278–296.
- Clancy, R. T. and Sandor, B. J. (1998). CO_2 ice clouds in the upper atmosphere of Mars. *Geophys. Res. Lett.*, 25:489–492.
- Clancy, R. T., Wolff, M. J., Whitney, B. A., Cantor, B. A., and Smith, M. D. (2007). Mars equatorial mesospheric clouds: Global occurrence and physical properties from Mars Global Surveyor Thermal Emission Spectrometer and Mars Orbiter Camera limb observations. *Journal of Geophysical Research (Planets)*, 112(E11):4004+.
- Creasey, J. E., Forbes, J. M., and Hinson, D. P. (2006). Global and seasonal distribution of gravity wave activity in Mars’ lower atmosphere derived from MGS radio occultation data. *Geophys. Res. Lett.*, 33:1803.
- Fritts, D. and Alexander, M. (2003). Gravity wave dynamics and effects in the middle atmosphere. *Rev. Geophys.*, 41(1):1003.
- González-Galindo, F., Forget, F., López-Valverde, M. A., Angelats i Coll, M., and Millour, E. (2009). A Ground-to-Exosphere Martian General Circulation Model. I. Seasonal, Diurnal and Solar Cycle Variation of Thermospheric Temperatures. *Journal of Geophysical Research (Planets)*, in press.
- González-Galindo, F., Määttänen, A., Forget, F., and Spiga, A. (2011). The martian mesosphere as revealed by CO_2 clouds observations and general circulation modeling. Submitted to *Icarus*.
- Hauchecorne, A., Chanin, M. L., and Wilson, R. (1987). Mesospheric temperature inversion and gravity wave breaking. *Geophys. Res. Lett.*, 14:933–936.
- Lindzen, R. S. (1981). Turbulence and stress owing to gravity wave and tidal breakdown. *J. Geophys. Res.*, 86:9707–9714.
- Määttänen, A., Montmessin, F., Gondet, B., Scholten, F., Hoffmann, H., González-Galindo, F., Spiga, A., Forget, F., Hauber, E., Neukum, G., Bibring, J., and Bertaux, J. (2010). Mapping the mesospheric CO_2 clouds on Mars: MEX/OMEGA and MEX/HRSC observations and challenges for atmospheric models. *Icarus*, 209:452–469.
- Magalhaes, J. A., Schofield, J. T., and Seiff, A. (1999). Results of the Mars Pathfinder atmospheric structure investigation. *J. Geophys. Res.*, 104:8943–8956.
- McConnochie, T. H., Bell, J. F., Savransky, D., Wolff, M. J., Toigo, A. D., Wang, H., Richardson, M. I., and Christensen, P. R. (2010). THEMIS-VIS observations of clouds in the martian mesosphere: Altitudes, wind speeds, and decimeter-scale morphology. *Icarus*, 210:545–565.
- Millour, E., Forget, F., and Lewis, S. R. (2008). Mars Climate Database v4.3 Detailed Design Document, available on <http://web.lmd.jussieu.fr/forget/dvd/docs>.
- Montmessin, F., Bertaux, J.-L., Quémérais, E., Korabiev, O., Rannou, P., Forget, F., Perrier, S., Fussen, D., Lebonnois, S., Rébérac, A., and Dimarellis, E. (2006). Subvisible CO_2 ice clouds detected in the mesosphere of Mars. *Icarus*, 183:403–410.
- Montmessin, F., Gondet, B., Bibring, J.-P., Langevin, Y., Drossart, P., Forget, F., and Fouchet, T. (2007). Hyperspectral imaging of convective CO_2 ice clouds in the equatorial mesosphere of Mars. *Journal of Geophysical Research (Planets)*, 112:11+.
- Parish, H. F., Schubert, G., Hickey, M. P., and Walterscheid, R. L. (2009). Propagation of tropospheric gravity waves into the upper atmosphere of Mars. *Icarus*, 203:28–37.
- Spiga, A. and Forget, F. (2009). A new model to simulate the Martian mesoscale and microscale atmospheric circulation: Validation and first results. *Journal of Geophysical Research (Planets)*, 114(E13):2009+.
- Withers, P. and Catling, D. C. (2010). Observations of atmospheric tides on Mars at the season and latitude of the Phoenix atmospheric entry. *Geophys. Res. Lett.*, 37:24204+.